Imaging mass spectrometry of intraspecies metabolic exchange revealed the cannibalistic factors of *Bacillus subtilis*

Wei-Ting Liu[a,1], Yu-Liang Yang[b,1], Yuquan Xu[b,1], Anne Lamsa[c], Nina M. Haste[b,d], Jane Y. Yang[a], Julio Ng[e], David Gonzalez[a], Craig D. Ellermeier[f], Paul D. Straight[g], Pavel A. Pevzner[e,h], Joe Pogliano[c], Victor Nizet[b,d,i], Kit Pogliano[c], and Pieter C. Dorrestein[a,b,d,2]

[a]Department of Chemistry and Biochemistry, [b]Skaggs School of Pharmacy and Pharmaceutical Sciences, [c]Division of Biological Sciences, [d]Center for Marine Biotechnology and Biomedicine, and [e]Department of Computer Science, University of California at San Diego, La Jolla, CA 92093; [f]Department of Microbiology, University of Iowa, Iowa City, IA 52242; [g]Department of Biochemistry and Biophysics, Texas A&M University, College Station, TX 77843; and [h]National Center for Research Resources (NCRR) Center for Computational Mass Spectrometry and [i]Department of Pediatrics, University of California at San Diego, La Jolla, CA 92093

Edited by Richard M. Losick, Harvard University, Cambridge, MA, and approved August 4, 2010 (received for review June 14, 2010)

During bacterial cannibalism, a differentiated subpopulation harvests nutrients from their genetically identical siblings to allow continued growth in nutrient-limited conditions. Hypothesis-driven imaging mass spectrometry (IMS) was used to identify metabolites active in a *Bacillus subtilis* cannibalism system in which sporulating cells lyse nonsporulating siblings. Two candidate molecules with sequences matching the products of *skfA* and *sdpC*, genes for the proposed cannibalistic factors sporulation killing factor (SKF) and sporulation delaying protein (SDP), respectively, were identified and the structures of the final products elucidated. SKF is a cyclic 26-amino acid (aa) peptide that is posttranslationally modified with one disulfide and one cysteine thioether bridged to the α-position of a methionine, a posttranslational modification not previously described in biology. SDP is a 42-residue peptide with one disulfide bridge. In spot test assays on solid medium, overproduced SKF and SDP enact a cannibalistic killing effect with SDP having higher potency. However, only purified SDP affected *B. subtilis* cells in liquid media in fluorescence microscopy and growth assays. Specifically, SDP treatment delayed growth in a concentration-dependent manner, caused increases in cell permeability, and ultimately caused cell lysis accompanied by the production of membrane tubules and spheres. Similarly, SDP but not SKF was able to inhibit the growth of the pathogens *Staphylococcus aureus* and *Staphylococcus epidermidis* with comparable IC_{50} to vancomycin. This investigation, with the identification of SKF and SDP structures, highlights the strength of IMS in investigations of metabolic exchange of microbial colonies and also demonstrates IMS as a promising approach to discover novel biologically active molecules.

cannibalism | bacterial communication | natural product | posttranslational modifications | thioether

Metabolic exchange describes the process of exchanging signals or nutrients between cells or populations and is a common feature of all living systems. Bacteria produce a wide array of signaling molecules to control metabolic as well as morphological and developmental changes in either an interspecies or intraspecies manner (1). *Bacillus subtilis,* for example, has a complex life cycle and thrives in diverse living conditions ranging from soil, contaminated wounds, and the intestinal tract (2–4). To accommodate this, *B. subtilis* dedicates ∼10% of its genome to the production of specific molecules involved in intra- and interspecies metabolic exchange (5). Two of these molecules are sporulation delaying protein (SDP) and sporulation killing factor (SKF), which, based on genetic experiments, are proposed to lyse a subpopulation of *B. subtilis* cells to provide nutrients for the remaining cells, a process referred to as bacterial cannibalism (6–10). This behavior is dependent on Spo0A, a master transcriptional regulator that also controls biofilm formation and sporulation (6–13). We set out to characterize these cannibalistic compounds to establish their roles in the *B. subtilis* life cycle and to understand their structure and biosynthesis. In addition, previous reports have suggested that the *skf* and *sdp* gene clusters preferentially target non-*B. subtilis* cells, suggesting that the cannibalistic factors might represent promising new antibiotic leads (14, 15).

Before this study, SDP had been partially purified (6), whereas SKF had not been identified or structurally characterized, although *B. subtilis* is the model organism for Gram-positive bacteria and many laboratories had investigated its metabolic output. The difficulties of identifying these molecules could arise from the fact that the cannibalistic effect was observed only on solid media but not in liquid media (6). Therefore, we decided to use imaging mass spectrometry (IMS) to visualize the process by growing the domesticated strain PY79 directly on the MALDI target plate (16–18). With this approach, we were able to purify and determine the structure of mature SKF and SDP. In solid medium, both molecules act as cannibalistic killing factors, however, only SDP inhibited the growth of *B. subtilis* and the Gram-positive pathogens *Staphylococcus aureus* and *Staphylococcus epidermidis* in liquid medium. This investigation demonstrates that IMS is an effective tool to identify cell-to-cell interaction signals, and provides an approach to the discovery of bioactive molecules.

Results and Discussion

Identification of SKF and SDP via IMS. The *B. subtilis* cannibalistic phenotype presents itself only on solid media (6), yet there are very few tools that can spatially characterize metabolic output on solid surfaces. We therefore used thin-layer agar IMS, which is capable of capturing the spatial distribution of metabolites in growing colonies and can be used to understand microbial metabolic exchange, to visualize the cannibalistic factors SKF and SDP (18). In this IMS experiment, a growing culture of *B. subtilis* PY79, used in the original report on cannibalism (6), was cultured adjacent to a Δ*spo0A* strain (KP648) and its metabolic output was profiled by IMS (Fig. 1*A*). We anticipated that a zone of clearing on the Δ*spo0A* strain would be observed and that IMS could be used to

Author contributions: C.D.E., P.D.S., P.A.P., J.P., V.N., K.P., and P.C.D. designed research; W.-T.L., Y.-L.Y., Y.X., A.L., N.M.H., J.Y.Y., J.N., D.G., C.D.E., J.P., and K.P. performed research; W.-T.L., Y.-L.Y., Y.X., A.L., N.M.H., J.Y.Y., J.N., D.G., J.P., K.P., and P.C.D. analyzed data; and W.-T.L., Y.-L.Y., K.P., and P.C.D. wrote the paper.

The authors declare no conflict of interest.

This article is a PNAS Direct Submission.

Freely available online through the PNAS open access option.

[1]W.-T.L, Y.-L.Y, and Y.X. contributed equally to this work.

[2]To whom correspondence should be addressed. E-mail: pdorrest@ucsd.edu.

This article contains supporting information online at www.pnas.org/lookup/suppl/doi:10.1073/pnas.1008368107/-/DCSupplemental.

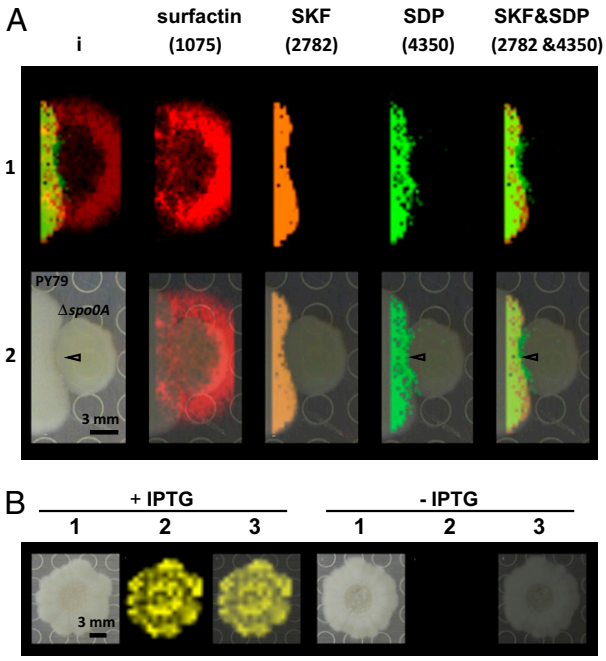

Fig. 1. IMS of intraspecies metabolic exchange. (*A*) IMS of PY79 and Δ*spo0A* (KP648) coculture. (*1*) Ion distributions observed for surfactin ($[M+K]^+$), SKF ($[M+H]^+$), and SDP ($[M+K]^+$). *1i* is a superimposition of all three ions. (*2*) Superimposition of the photograph and IMS data. Arrows point to glassy region of Δ*spo0A* and SDP overlap. (*B*) IMS of EG208 with or without IPTG. (*1*) Photographs of the colonies. (*2*) IMS pictures of ion 2782. (*3*) Superimposition of *1* and *2*.

identify candidate signals involved in the lysis of Δ*spo0A* cells. Indeed, we observed a decreased growth phenotype as well as a glassy appearance in the region of Δ*spo0A* adjacent to the cocultured PY79 cells (Fig. 1*A* and *SI Appendix*, Fig. S1).

Several ions were observed in the IMS data. First, KP648 (PY79, Δ*spo0A*) produced the nonribosomal peptide synthetase-derived lipopeptide antibiotic surfactin. This was unexpected, because PY79 has a frameshift mutation in the gene encoding for the phosphopantetheinyl transferase protein, Sfp (19), and we confirmed by DNA sequencing that this mutation is present in the Δ*spo0A* strain. This indicates that the surfactin nonribosomal peptide synthetases are activated via a lower efficiency phosphopantetheinylation pathway that is up-regulated in the absence of Spo0A. However, judging from their relative mass spectrometry (MS) intensities, the signal of surfactin at 96 h was at least 10-fold less than the amount produced by the nondomesticated *B. subtilis* strain 3610 (*SI Appendix*, Fig. S2), which has a functional *sfp* gene. Second, some signals produced by PY79 appeared to define a boundary between the PY79 and Δ*spo0A* colonies, including the ions at *m/z* 2782 and 4350 (Fig. 1*A*). Ion 2782 was associated with the border between the two cultures, and ion 4350 was found in the regions where the Δ*spo0A* strain was glassy and displayed reduced growth. Thus, the 4350 *m/z* ion was the favored candidate that caused the majority of the cannibalistic killing effect, because of the overlap with the zone of reduced growth on Δ*spo0A*, whereas the 2782 ion stopped at the interface of the two colonies.

After an l-butanol extraction and a desalting step, the two uncharacterized ions were measured at *m/z* 2782 $[M+H]^+$ and 4312 $[M+H]^+$, suggesting that ion *m/z* 4350 is the potassium adduct form $[M+K]^+$ (*SI Appendix*, Fig. S3). These two ions were then subjected to fragmentation by MALDI-TOF tandem MS (TOF/TOF). The ion at *m/z* 4312 $[M+H]^+$ gave a long and unambiguous sequence tag corresponding to VAAGYLYVVGVNAVALQT-AAAVTTAVW and matched residues from Val^{148} to Trp^{174} of SdpC (*SI Appendix*, Figs. S4*A* and S5 and Table S1), whereas the TOF/TOF fragmentation of the 2782 ion gave a candidate sequence tag, LPHPA (*SI Appendix*, Fig. S4*B*). This sequence tag matched a sequence within SkfA, the proposed precursor for the mature form of SKF (6). However, the sequence tag was insufficient to positively identify SKF, because none of the ion masses could be directly matched with the linear sequence of SkfA, and many ions in the spectrum remained unexplained. To confirm the identity of this ion, strain EG208 with an IPTG inducible promoter in front of the *skf* gene cluster was subjected to IMS. If the ion with *m/z* of 2782 is SKF, it is expected to be present only when IPTG is added. Indeed, in the absence of IPTG, the ion at *m/z* 2782 is absent as judged by IMS (Fig. 1*B*). In addition, the production of this ion was abolished when the *skfA* gene was inactivated, solidifying that this 2782 ion is indeed the mature form of SKF (*SI Appendix*, Fig. S2, EG165). Similarly, the 4350 signal was not observed in an *sdpC* deletion strain, in agreement with the identification of this ion as SDP (*SI Appendix*, Fig. S2, EH273).

Isolation and Structural Elucidation of SDP and SKF. With the masses of SKF and SDP in hand, it became possible to use an MS-guided isolation for both molecules. Unlike the antibiotics surfactin and subtilosin, SDP and SKF did not readily diffuse into the solid media as judged by IMS (Fig. 1*A* and *B* and *SI Appendix*, Fig. S2). This implied that SDP and SKF are hydrophobic in nature, and thus we adapted our purification protocol accordingly (*SI Appendix, SI Methods*). The isolation and subsequent structural analysis using tandem MS and NMR enabled us to determine that SDP is a 42-aa peptide with a disulfide crosslink and that SKF is a 26-aa

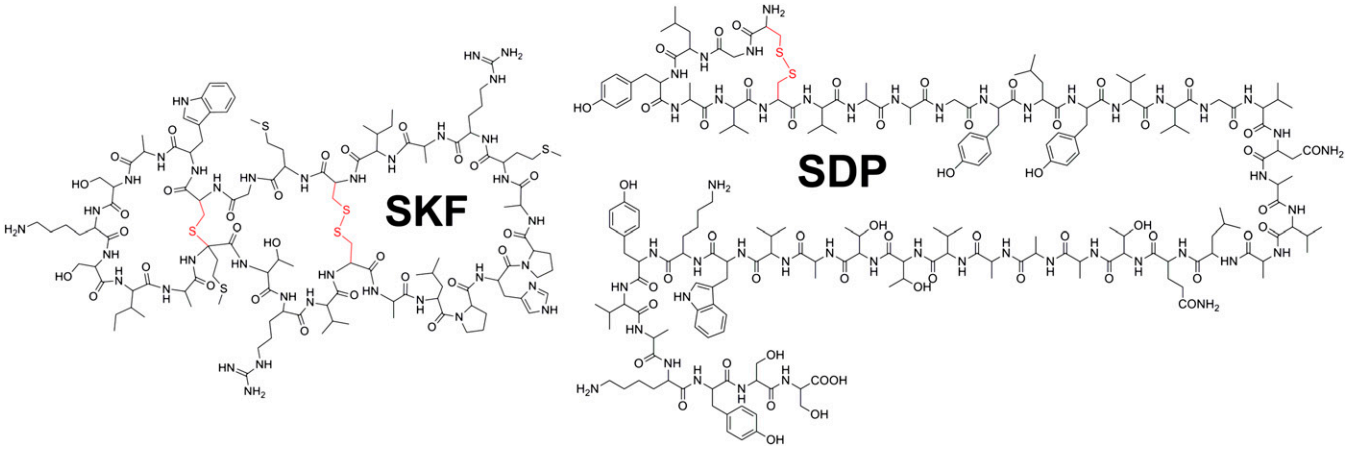

Fig. 2. Structures of SKF and SDP.

disulfide-containing cyclic peptide with a thioether crosslink of a cysteine to the α-carbon of a methionine (Fig. 2). This ribosomally encoded peptide is unusual in terms of structure but is consistent with the transport and biosynthetic enzymes found on the *skf* gene cluster as described in *SI Appendix, SI Text* (6). A full description of the data and methods that led us to the determination of these structures is provided in *SI Appendix, SI Text*.

Biological Effects of SDP and SKF. With the availability of microgram quantities of purified SKF and SDP, the biological effects of these compounds on *B. subtilis* growth in liquid and solid cultures and the effects on cell structure were evaluated. First, we added the purified compounds to liquid cultures of the undomesticated WT strain 3610, its domesticated laboratory descendent PY79, and a PY79 strain containing the Δ*spo0A* mutation (KP648). 3610 was included to verify the relevance of our findings to an undomesticated strain of *B. subtilis*. In rich media (ISP2 or LB media), 20 μg/mL purified SDP significantly and rapidly inhibited growth of 3610, PY79, and Δ*spo0A*, whereas 20 μg/mL SKF, surprisingly, had little observable effect on growth (*SI Appendix*, Fig. S6). PY79 was much less affected by the addition of SDP than the other strains, presumably because PY79 produces SKF and SDP during growth and likely expresses the resistance genes, whereas we were unable to detect the compounds in the Δ*spo0A* mutant under any conditions tested and 3610 produced low levels of the compounds only at late times on LB and DSM (*SI Appendix*, Figs. S2 and S7).

To determine the growth inhibitory activity of SDP in more detail, we investigated the effects of different concentrations of SDP on growth of the Δ*spo0A* strain KP648. A concentration-dependent growth effect was observed (Fig. 3*A*). Upon addition of 5–20 μg/mL SDP, growth was halted but was able to resume after several hours of continued incubation. The recovery represents survival of a subpopulation of SDP-resistant cells that are able to resume growth after a lag period (discussed below). The concentration of SDP significantly affected the degree to which growth was inhibited and the length of the growth lag. To evaluate how

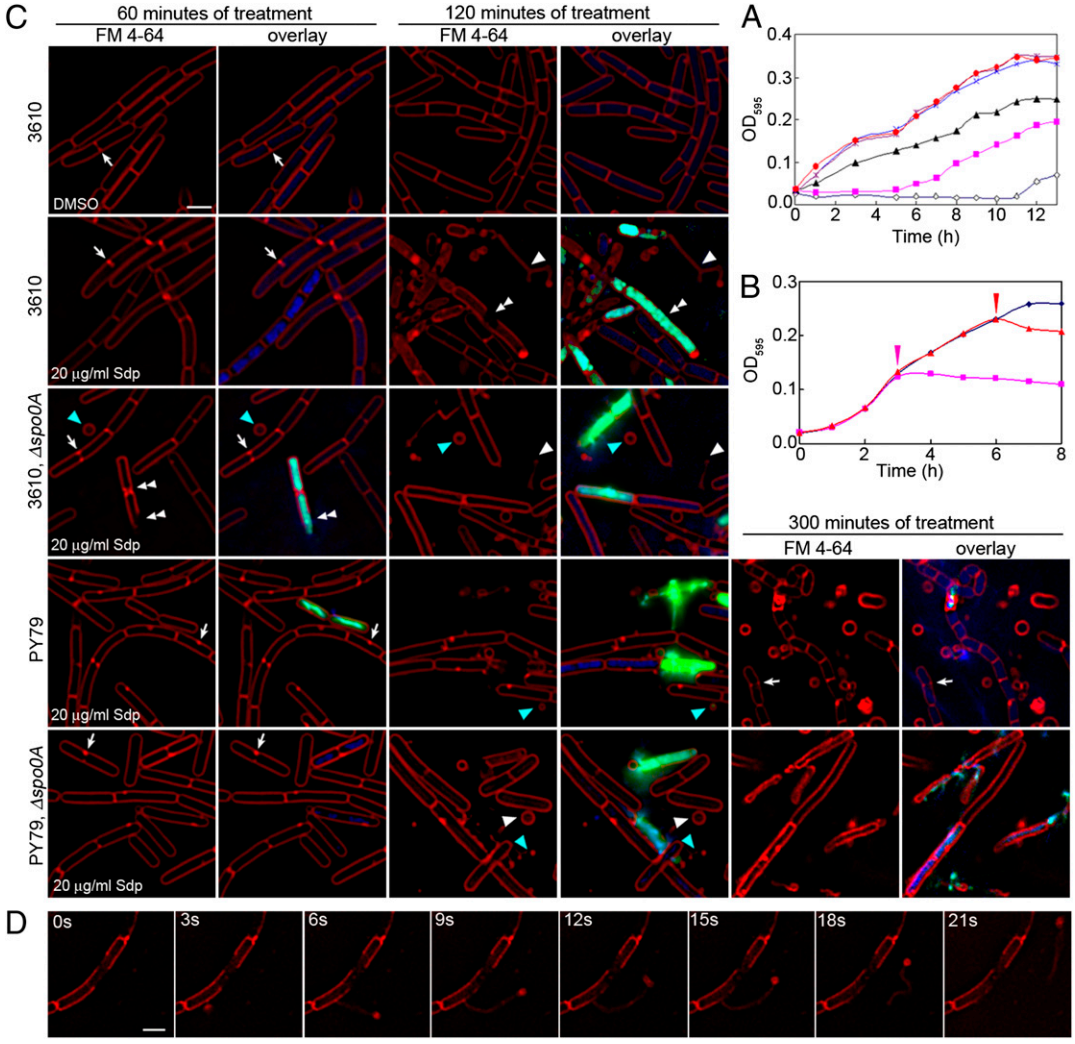

Fig. 3. Biological effects of SDP on *B. subtilis*. (*A*) Growth curves of KP648 (Δ*spo0A*) in ISP2 media with various concentration of SDP. SDP was added at 0 h. Indicates 20 μg/mL; . 10 μg/mL; , 5 μg/mL; , 2 μg/mL; , 0.2 μg/mL; and , DMSO control. (*B*) Growth curves of KP648 (Δ*spo0A*) in ISP2 media with 20 μg/mL SDP. SDP was added at 3 h ( ) and 6 h ( ). Indicates DMSO control. (*C*) Fluorescence micrographs of growing cells of 3610, PY79, ALB1035 (3610, Δ*spo0A*), and KP648 (PY79, Δ*spo0A*) treated with DMSO or 20 μg/mL SDP for the time indicated. Red stain is FM 4–64, a fluorescent membrane stain; blue and green stains are DAPI and Sytox Green, two DNA stains that are membrane impermeable. Sytox Green is the least permeable and provides the greatest increase in fluorescence in permeabilized cells. White arrows point to dividing cells. In the DMSO control, the arrow points to a normal division, whereas in the other images the septa are asymmetric. Double arrowheads point to large gaps in membrane staining. Light blue triangles point to membrane spheres, whereas white triangles point to tubular membranes. After 300 min of treatment of PY79 with SDP, surviving cells are smaller, dividing, and impermeable to Sytox. (*D*) Time-lapse microscopy images collected at 110 min after SDP treatment. Still images from 0 to ~21 s are shown.

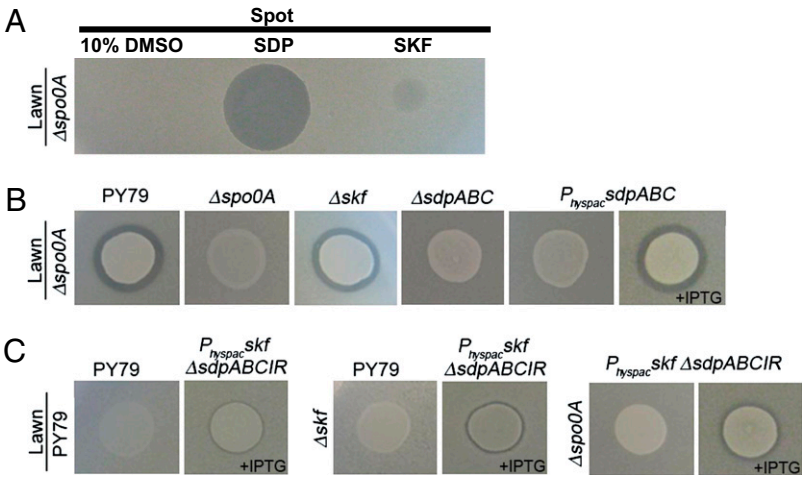

Fig. 4. Spot assays to compare the effect of exogenously supplied and endogenously produced SDP and SKF. Lawns of indicated strains were prepared in top agar. After solidification, the lawns were spotted with either (*A*) purified SDP, SKF, and DMSO or (*B*,*C*) the indicated strains that overexpress or lack SDP and SKF.

rapidly SDP inhibited growth, SDP was added to an exponentially growing culture. The addition of 20 μg/mL SDP at different time points rapidly caused growth to level off with very little decrease in optical density (Fig. 3*B*). These results demonstrate that purified SDP has rapid effects on growth of *B. subtilis* cells but that SKF does not at the highest concentration (20 μg/mL) that we tested.

We next performed fluorescence microscopy on living cells of 3610, PY79, and the Δ*spo0A* derivatives of these strains (ALB1035 and KP648, respectively) following treatment with 20 μg/mL SDP for various times in liquid culture. Cells were stained with FM 4–64, a fluorescent membrane stain that inserts into the outer leaflet of the bilayer, as well as Sytox Green and DAPI, two DNA stains that do not efficiently cross the bilayer unless the cells are permeabilized (Fig. 3*C*). The first effect was noted ≈60 min after the addition of SDP to 3610, when we observed that the cells often showed partial, asymmetric septa, and localized bright staining of membranes (arrows), suggesting the presence of deformations in the cytoplasmic membrane, particularly at division sites. Approximately 5% of the cells at this time also showed increased permeability to Sytox Green and DAPI, and a subset of these cells showed large gaps in the membrane staining (double arrowheads), suggesting that these cells lack an intact cytoplasmic membrane. By 120 min, more cells showed increased permeability to Sytox Green, DAPI, and discontinuous membranes, and we observed many spherical and tubular membrane projections (arrowheads). By 120 min, ~33% of all morphologically intact 3610 cells stained with Sytox Green, indicating they were permeablized, and 5% of the cells had protruding tubules (*SI Appendix*, Tables S2 and S3). By 300 min, very few intact cells remained in the Δ*spo0A* culture, whereas the PY79 culture still contained dividing cells, confirming the increased sensitivity of the Δ*spo0A* mutant to SDP. Time-lapse microscopy revealed that the membrane tubules were formed and released in a matter of seconds (Fig. 3*D* and Movie S1).

The domesticated strain PY79 and its Δ*spo0A* derivative (KP648) responded more slowly to SDP, with only ~4% of cells showing increased Sytox Green permeability at 60 min after treatment, and with major changes in cell morphology first observed 90 min after treatment. At 120 min, 13.7% of all morphologically intact PY79 cells stained with Sytox and increased to 19.8% in the PY79, Δ*spo0A* strain (*SI Appendix*, Table S2). These results confirm our initial hypothesis that the 4350 *m/z* ion, due to the overlap with the decreased growth phenotype of Δ*spo0A* in the coculture of Δ*spo0A* with PY79, is the major cannibalistic factor. Furthermore, the data indicate that SDP does not rapidly lyse all of the Spo0A-OFF cells and that a subpopulation of Δ*spo0A* cells remains viable even after several hours of treatment, suggesting an additional degree of multicellular behavior in a population of genetically identical *B. subtilis* cells.

Dual Nature of SKF- and SDP-Mediated Killing of Sister Cells. Having failed to detect any biological affect of purified SKF using the above liquid culture assays, we wanted to evaluate the ability of SKF and SDP to work independently on solid media. To assess this, we set out to determine whether purified SDP or SKF inhibited the growth of Δ*spo0A* on solid media. Spotting 2 μg SDP resulted in a large zone of decreased growth, and 2 μg SKF resulted in a smaller zone in which the lawn appeared somewhat thinner, whereas the control 10% DMSO did not have an effect on the growth (Fig. 4*A*). This indicates that both SDP and SKF reduce the growth of *B. subtilis* on solid media, although purified SDP has a much stronger effect than SKF.

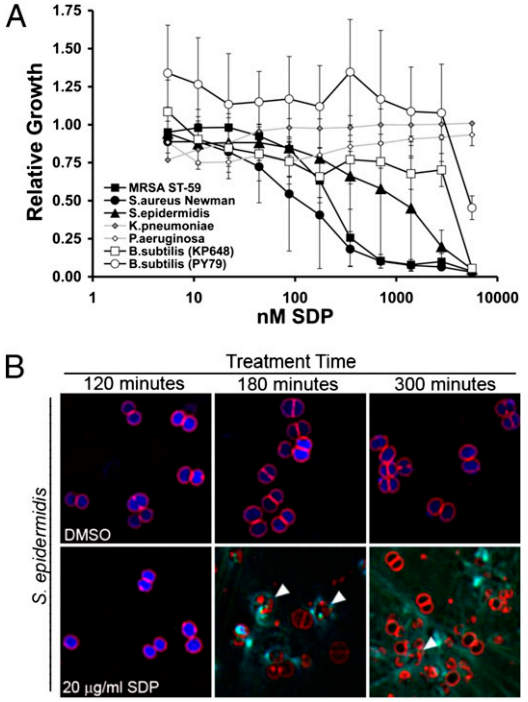

Fig. 5. Biological activity of SDP on clinically relevant human pathogens. (*A*) SDP inhibition curves for pathogenic microbes. Relative growth of *P. aeruginosa*, *K. pneumoniae*, *B. subtilis* strains KP648 (Δ*spo0A*), and PY79, *S. aureus* Newman strain, a clinical isolate of methicillin-resistant *S. aureus*, and *S. epidermidis* with the presence of increasing concentrations of SDP is shown in the curve. (*B*) Fluorescence micrograph showing growing cells of *S. epidermidis* treated with DMSO or 20 μg/mL SDP in DMSO for the time indicated and stained with FM 4–64 (red), DAPI (blue), and Sytox (green), as in Fig. 3.

We next sought to determine whether SDP and SKF produced independent killing effects of similar magnitude when overproduced on solid medium. To do so, we used a spot assay in which PY79, Δ*spo0A,* Δ*skf*, Δ*sdp,* and SKF- or SDP-overexpressing strains are spotted on *B. subtilis* lawns. When PY79 was spotted on the Δ*spo0A* lawn, a large zone of clearing was observed (Fig. 4*B*), as previously reported (6). This phenomenon is mostly dependent on SDP, as the inhibitory effect was still observed with a Δ*skf* strain but was abolished when *sdpABC* genes were deleted or not induced (Fig. 4*B*). We next overexpressed SKF in an *sdpABCIR* deletion background to eliminate the effect of SDP (P_{hyspac}*skf,* Δ*sdpABCIR*), and observed a killing effect toward lawns of PY79, Δ*skf* and Δ*spo0A* (Fig. 4*C*). These results indicate that although most of the killing effect of PY79 on a Δ*spo0A* lawn is mediated by SDP rather than SKF, overexpression of the *skf* operon still mediates a killing activity. Thus, either SKF or SDP can independently mediate cannibalism on solid culture medium, but SDP is much more potent than SKF.

SDP but Not SKF Has Antibacterial Activities Against Pathogens. The above results indicate that both SKF and SDP mediate cannibalistic effects. We therefore set out to determine whether these two molecules would also display activity against human pathogens by screening purified SKF and SDP for inhibitory activity against a panel of pathogenic microbes (including *B. subtilis* strains PY79 and its Δ*spo0A* derivative for comparison). We used a growth assay that measures differences in cell density compared with untreated controls. This screen revealed that SKF had no effect on growth, whereas SDP decreased cell density of members of the Gram-positive genus *Staphylococcus* to a greater extent than *B. subtilis,* but it did not affect the tested Gram-negative pathogens *Pseudomonas aeruginosa* or *Klebsiella pneumoniae* (Fig. 5*A*). SDP exhibited potent inhibitory activity against two *S. aureus* variants, the Newman strain used extensively in laboratory studies of *S. aureus* virulence, as well as a clinical isolate of methicillin-resistant *S. aureus* (MRSA) sequence type ST59. The IC_{50} against these *S. aureus* strains were 210 and 110 nM, respectively, slightly more active than the leading contemporary pharmacological agent for treatment of MRSA infection, vancomycin (IC_{50} 360, 270 nM, respectively). SDP also inhibited growth of *S. epidermidis*, an opportunistic pathogen associated with nosocomial infections of catheters and the urinary tract and invasive infections in human premature neonates (IC_{50} 990 nM). SDP has a relatively simple chemical structure, and might therefore provide an antibiotic candidate for future development of derivatives with smaller size and optimized activity against MRSA and closely related species.

In summary, this paper highlights the need for the development of new technologies to study and discover biologically active molecules, a cornerstone of chemical biology as well as therapeutic discovery (20). Thin-layer agar MALDI-IMS of cocultures of bacterial colonies enabled the discovery, isolation, and structural elucidation of two biologically active factors, SKF and SDP, one of which was cyclized and uniquely posttranslationally modified with a thioether linkage to the α-position of a methionine. MALDI-IMS can also be used to predict the function of metabolites. In this study, we observed an overlap of SDP extending from the cocultured strain PY79 with the region of Δ*spo0A* that was inhibited, enabling us to formulate a hypothesis that SDP, but not SKF, was the main cannibalistic factor. Indeed, when we tested the biological activities of the purified compounds, only SDP showed inhibitory activity in liquid cultures. On the other hand, both SDP and SKF mediated inhibition on solid cultures when overexpressed in whole cells grown on solid medium or when the purified compounds were spotted onto solid media. However, SKF, was much less potent than SDP, and our data indicate that SDP is the primary toxin that mediates cannibalism. Finally, screening both SKF and SDP for their antibacterial activities allowed us to demonstrate that SDP, but not SKF, inhibits growth of *Staphylococci* to a greater extent than it inhibits *B. subtilis* growth. This suggests that SDP also participates in defensive or predatory behavior directed at other species (14, 15), as well as cannibalism (6). The fact that SDP inhibited clinically relevant pathogens also demonstrates a unique application of studying metabolic exchange by IMS in the discovery of biologically active molecules, and therefore represents that IMS can be used as a tool in efforts to discover new classes of therapeutic agents.

Methods

Structural elucidation of SKF and SDP, as well as the annotation of SKF biosynthetic gene cluster, are described in *SI Appendix, SI Text*. Details regarding strains, culture conditions, bioassays are provided in *SI Appendix, SI Methods*. The procedures used in thin-layer agar MALDI IMS, purification of SKF and SDP, SKF derivatization, MS, NMR, and fluorescence microscopy are also detailed in *SI Appendix, SI Methods*.

ACKNOWLEDGMENTS. We thank the staff at the Losick laboratory (Harvard University, Cambridge, MA) for providing *skf* and *sdp* mutant strains, Michael Fischbach (University of California San Francisco, San Francisco, CA) for providing the *S. epidermidis* strain, and William H. Gerwick (University of California San Diego, La Jolla, CA) for critically reviewing the manuscript. Funding for the Dorrestein laboratory was provided by the Beckman Foundation and National Institute of General Medical Sciences Grant NIHGM086283 (to P.C.D. and P.A.P.). W.-T.L. was supported in part by study abroad Grant SAS-98116-2-US-108 from Taiwan. N.M.H and J.Y.Y. were supported by Ruth L. Kirschstein National Research Service Award (NRSA) from National Institutes of Health Grants 1 F31 GM90658-01 and 1 T32 EB009380-01, respectively. P.A.P. was supported by the National Center for Research Resources of National Institutes of Health via Grant P-41-RR024851. Funding for the Joe Pogliano lab was provided by National Institute of General Medical Sciences Grant NIHGM073898. Funding for the Kit Pogliano laboratory was provided by National Institute of General Medical Sciences Grant NIHGM57045.

1. Shank EA, Kolter R (2009) New developments in microbial interspecies signaling. *Curr Opin Microbiol* 12:205–214.
2. Tam NKM, et al. (2006) The intestinal life cycle of *Bacillus subtilis* and close relatives. *J Bacteriol* 188:2692–2700.
3. Aguilar C, Vlamakis H, Losick R, Kolter R (2007) Thinking about *Bacillus subtilis* as a multicellular organism. *Curr Opin Microbiol* 10:638–643.
4. Earl AM, Losick R, Kolter R (2008) Ecology and genomics of *Bacillus subtilis*. *Trends Microbiol* 16:269–275.
5. Kunst F, et al. (1997) The complete genome sequence of the gram-positive bacterium *Bacillus subtilis*. *Nature* 390:249–256.
6. González-Pastor JE, Hobbs EC, Losick R (2003) Cannibalism by sporulating bacteria. *Science* 301:510–513.
7. Ellermeier CD, Hobbs EC, Gonzalez-Pastor JE, Losick R (2006) A three-protein signaling pathway governing immunity to a bacterial cannibalism toxin. *Cell* 124:549–559.
8. Engelberg-Kulka H, Amitai S, Kolodkin-Gal I, Hazan R (2006) Bacterial programmed cell death and multicellular behavior in bacteria. *PLoS Genet* 2:e135.
9. Claverys JP, Håvarstein LS (2007) Cannibalism and fratricide: Mechanisms and raisons d'être. *Nat Rev Microbiol* 5:219–229.
10. López D, Vlamakis H, Losick R, Kolter R (2009) Cannibalism enhances biofilm development in *Bacillus subtilis*. *Mol Microbiol* 74:609–618.
11. Burbulys D, Trach KA, Hoch JA (1991) Initiation of sporulation in *B. subtilis* is controlled by a multicomponent phosphorelay. *Cell* 64:545–552.
12. Fawcett P, Eichenberger P, Losick R, Youngman P (2000) The transcriptional profile of early to middle sporulation in *Bacillus subtilis*. *Proc Natl Acad Sci USA* 97:8063–8068.
13. Molle V, et al. (2003) The Spo0A regulon of *Bacillus subtilis*. *Mol Microbiol* 50:1683–1701.
14. Lin D, Qu LJ, Gu H, Chen ZA (2001) A 3.1-kb genomic fragment of Bacillus subtilis encodes the protein inhibiting growth of Xanthomonas oryzae pv. oryzae. *J Appl Microbiol* 91:1044–1050.
15. Nandy SK, Bapat PM, Venkatesh KV (2007) Sporulating bacteria prefers predation to cannibalism in mixed cultures. *FEBS Lett* 581:151–156.
16. Cornett DS, Reyzer ML, Chaurand P, Caprioli RM (2007) MALDI imaging mass spectrometry: Molecular snapshots of biochemical systems. *Nat Methods* 4:828–833.
17. Seeley EH, Caprioli RM (2008) Molecular imaging of proteins in tissues by mass spectrometry. *Proc Natl Acad Sci USA* 105:18126–18131.
18. Yang YL, Xu Y, Straight P, Dorrestein PC (2009) Translating metabolic exchange with imaging mass spectrometry. *Nat Chem Biol* 5:885–887.
19. Zeigler DR, et al. (2008) The origins of 168, W23, and other *Bacillus subtilis* legacy strains. *J Bacteriol* 190:6983–6995.
20. Li JW, Vederas JC (2009) Drug discovery and natural products: End of an era or an endless frontier? *Science* 325:161–165.